

Evidence Reasoning Machine Based on DSMT for Mobile Robot Mapping in Unknown Dynamic Environment

Xinhan Huang, Peng Li, Min Wang
Department of Control Science and Engineering
Huazhong University of Science and Technology
Wuhan 430074, China

xhhuang@mail.hust.edu.cn, lipeng_hubei@126.com, wm526@163.com

Abstract - In this paper a new method of information fusion, Dezert-Smarandache Theory (DSMT) is introduced to deal with high conflicting and uncertain information. And then the Evidence Reasoning Machine (ERM) based on DSMT is presented for mobile robot mapping in unknown dynamic environment. Considering the characteristics of sonar sensors, the grid map method is adopted and a sonar sensor mathematical model is constructed based on DSMT. Meanwhile a few of general basic belief assignment functions (gbbaf) are constructed for fusion. Finally, map building experiment is carried out with Pioneer 2-DX mobile robot. The experiment results testify the validity of ERM with DSMT for fusing imprecise information during map building in unknown dynamic environment.

Keywords: Mobile robot, mapping, evidence reasoning, Dezert-Smarandache Theory.

1 Introduction

Mobile robot map building is an important topic in robotics research. Efficient exploration of an entirely unknown dynamic environment is a great difficulty for intelligent mobile robot. The robot has to deal with unexpected circumstances and require the ability to handle complex and rough environments with little or no prior knowledge of terrain. Robot obtains information of unknown environment and builds the environment map through their sensors such as sonar, laser, infrared, visual, etc. Ultrasonic range finders (sonar sensor) are mobile robots' most popular sensors due to their availability and low cost.

In unknown dynamic environment, there are too many uncertainties and conflicts. The most influencing factor is moving object, because it will cause high conflicting and uncertain information. And the accumulative substantial positional errors occur from the inertial or dead-reckoning navigation, especially for a long distance travel. For robot mapping, how to effectively filter these uncertainties is still a problem and a precise environment map cannot be built without solving the problem.

Robot mapping studies can fall into two subgroups. These are: (1) Grid based environment maps, (2) Object specification based maps. However most of these studies are concentrated on the first method. Noykov proposed a modified method for occupancy grid map built by a moving

mobile robot and a scanning ultrasonic range-finder [1]. Yenilmez used the sequential principal component (SPC) method to process sonar data [2]. Grisetti presented an approximate but highly efficient approach to mapping with Rao-Blackwellized particle filters [3]. In Momotaz's study, a novel method of integrating fuzzy logic (FL) and genetic algorithm (GA) were presented to solve the map building problem of mobile robots [4]. But these methods only faced the dynamic situations. Efficient mapping in unknown dynamic environment is still a problem. Furthermore, if an excellent method can deal with errors brought by sonar readings, sonar sensors not the expensive laser sensors can also be used to draw the dynamic environment maps accurately.

To deal with the high conflicting and uncertain information in unknown dynamic environment for robot mapping, a brand new information fusion method namely DSMT [5] which is an extension of Dempster-Shafer Theory (DST) [6] is introduced. The DSMT of plausible and paradoxical reasoning proposed in recent years allows to formally combine any types of independent sources of information represented in term of belief functions [7]. And then, the kernel of this system ---- ERM with DSMT is proposed.

2 Architecture of Evidence Reasoning Machine

2.1 Basic framework of ERM

Until now, there is no uniform architecture for evidence reasoning theories. So we propose an uniform architecture for evidence reasoning theories.

If all sources are reliable, the evidence reasoning theories usually can be divided into four layers: evidence source layer, belief assignment layer, belief fusion layer and decision-making layer. But most of the rules of combination proposed in these theories are based on the assumption of the same reliability of sources of evidence. When the sources are known not being equally reliable and the reliability of each source is perfectly known, it is natural and reasonable to discount each unreliable source proportionally to its corresponding reliability factor. Then a belief revision layer should be added between belief fusion layer and belief assignment layer (Shafer proposed discounting method to revise the assigned belief [7], but his

method can only deal with linear conditions). The basic framework of Evidence Reasoning Machine (ERM) is shown in Figure 1. The belief fusion layer can adopt different algorithms of these evidence theories.

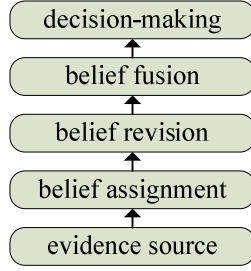


Figure 1 Basic framework of ERM

2.2 ERM based on DSMT

Because of the advantages DSMT, it is a good choice for ERM to make use of this algorithm. The ERM with two elements (θ_1, θ_2) based on DSMT is shown in Fig.2. In the belief assignment layer, the $F(S)$ is the belief assignment function, through which the original basic belief assignments (bba) $O(\cdot)$ are calculated. In the belief revision layer, instead of discounting method proposed by Shafer, the artificial neural network (ANN) is adopted. For under most conditions, the discounting values are unknown and nonlinear, but Shafer's discounting method is linear and the discounting values are fixed. The ANN is more flexible, it can learn of the nonlinear discounting curves through the foregone data, so it can depict the discounting situations more precisely than Shafer's method.

The $m(\cdot)$ is the bba revised by ANN. \otimes is multiplication operator. The $g(\cdot)$ is actuating function. For DSMT, this function is a simple sum operator; it can be rewritten for other evidence theory such as DST. $m_{M(\Theta)}(\cdot)$ is the fusion result. The PCR is proportional conflict redistribution rule. The conflict factor can be reassigned to $m_{M(\Theta)}(\theta_1)$ and $m_{M(\Theta)}(\theta_2)$, but if the conflict factor is not needed to be reassigned, it will directly become the $m_{M(\Theta)}(\theta_1 \cap \theta_2)$. The decision-making layer is an expanded layer if need. The probabilities of elements can be calculated through Generalized Pignistic Transformation (GPT). Usually this layer is not necessary. For the whole machine, though there are only two input evidence sources, it can deal with multi-source instances. Suppose a finite set of n sources $\{X_1, \dots, X_n\}$, in the beginning X_1 and X_2 is treated as S_1 and S_2 . After the first belief fusing cycle, the $m_{M(\Theta)}(\cdot)$ is got, but it is not the final result, so the $m_{M(\Theta)}(\cdot)$ returns and becomes the $m(\cdot)$ (it is treated as another S_1 and directly enters the belief fusion layer), and then X_3 participate in fusion, it is treated as another S_2 . After belief assigning and revising, the $m(\cdot)$ computed from X_3 will be fused with the $m(\cdot)$ converted directly from last fusion result $m_{M(\Theta)}(\cdot)$ and their fusion result will be treated as a source in the next fusion cycle. All of the sources can be processed in sequence. When

the final fusion result comes out, it can enter the final decision-making layer.

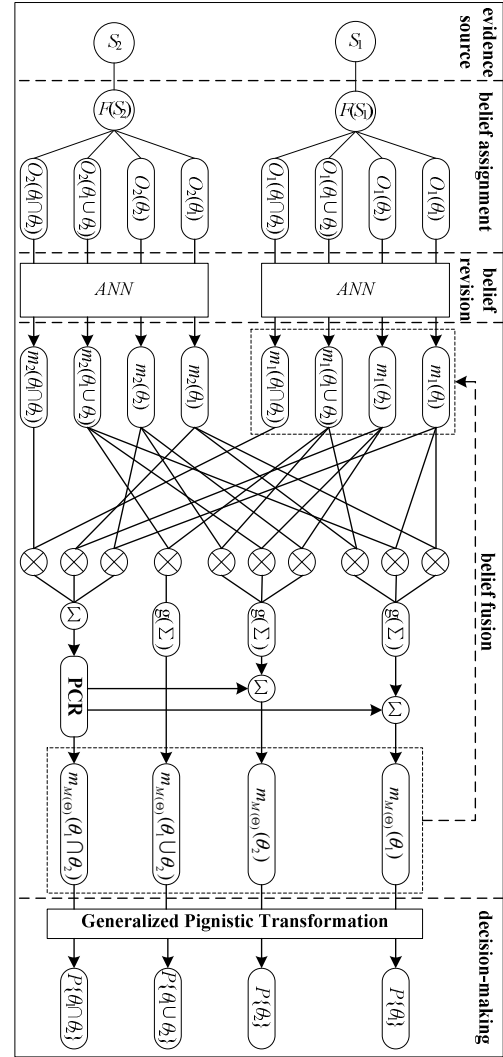


Figure 2 ERM based on DSMT

Under the two elements θ_1 and θ_2 condition, this ERM includes the classical DSMT model and the hybrid DSMT model. Of course if the amount of elements is more than two, the architecture of the belief fusion layer in this ERM is more complex. But under most conditions two elements are enough.

3 Sonar sensor modeling for DSMT

The simple principle of sonar sensor is: it generates sheaves of cone-shaped wave to detect the objects. The wave will be reflected as soon as it encounters an object. Since the sound wave generated by sonar sensor spreads forwards in the form of loudspeaker, there exists a divergence angle. Any object in the fan-shaped area can reflect the wave, so the real position of the objects detected among the fan-shaped area cannot be clearly known. And there are many other environment influences, so the data obtained by sonar sensor is not accurate. The beam angle of sonar ultrasonic is 15 degrees, which has been proved in our experiments. The

range of sonar readings is from 10 centimeters to nearly 5 meters.

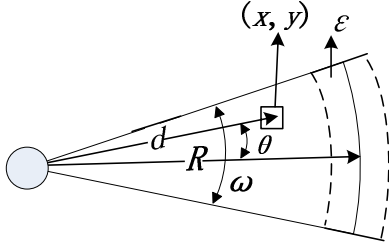


Figure 3 Sonar model based on DSMT

According to characteristics of sonar sensor, we construct a mathematic model of sonar sensor (shown in Figure 3.) based on DSMT to solve the problem. Suppose there are two elements θ_1 and θ_2 in the frame of discernment . Here the is defined as the status of each grid on the map constructed by the robot.

θ_1 means the grid in map is empty, θ_2 means occupied by some objects, $\theta_1 \cap \theta_2$ means the grid cannot be clearly ascribed to empty state or occupied state, it is the conflict mass generated by the computation of information fusion, and $\theta_1 \cup \theta_2$ means that information about the grid is unknown. The hyper-power set of the discernment frame is $D = \{\phi, \theta_1 \cap \theta_2, \theta_1, \theta_2, \theta_1 \cup \theta_2\}$. Then $m(\theta_1)$ denotes the general basic belief assignment functions (gbbaf) for the empty status, define $m(\theta_2)$ as the gbbaf for occupied status, $m(\theta_1 \cap \theta_2)$ is considered as the gbbaf of conflict mass, and $m(\theta_1 \cup \theta_2)$ is defined as the gbbaf of unknown status (it mainly refers to those areas that are still not scanned at present).

The belief assignments $m(\cdot): D \rightarrow [0,1]$ are constructed by authors such as the formulas (1) ~ (5) according to the sonar based on DSMT [8]:

$$m(\theta_1) = (1 - \frac{\lambda}{2}) \cdot \exp[\frac{-d^2}{2(R\rho_E)^2}], \quad R_{\min} \leq d \leq R + 2\epsilon; \quad (1)$$

$$m(\theta_2) = \lambda \cdot \exp[\frac{-(d-R)^2}{2R\rho_O^2}], \quad R_{\min} \leq d \leq R + 2\epsilon; \quad (2)$$

$$m(\theta_1 \cap \theta_2) = \exp[-\rho_C(\ln d - \beta)^2], \quad R_{\min} \leq d \leq R + 2\epsilon; \quad (3)$$

$$m(\theta_1 \cup \theta_2) = \begin{cases} (1 - \lambda) \cdot \tanh\{\frac{\rho_I[d - (R + \epsilon)]}{R}\}, & R + \epsilon \leq d \leq R + 2\epsilon \\ 0 & \text{, other ;} \end{cases} \quad (4)$$

$$\beta = \ln(\frac{\rho_E \sqrt{R^3}}{\rho_E \sqrt{R} + \rho_O}) \quad (5)$$

$$\lambda = \begin{cases} 1 - (\frac{2\theta}{\omega})^2 & 0 \leq \theta \leq \frac{\omega}{2}, \\ 0 & \text{other.} \end{cases} \quad (6)$$

The Eq.(6) is given by reference [9]. Here R_{\min} is the minimum sonar reading that sonar can obtain. R is the sonar reading between sonar and object. d is the distance from sonar to the point (x, y) in the map. ω is the divergence

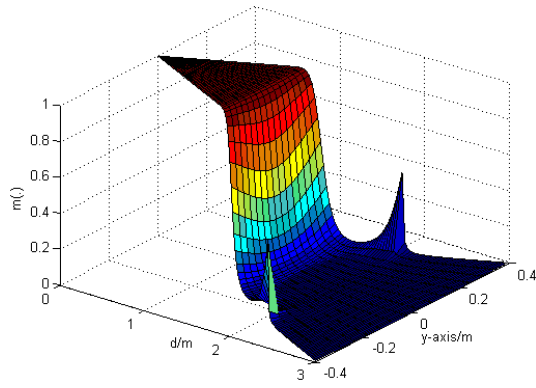
angle defined as 15 degrees. is the angle between d and axis. ϵ is the error of sonar reading and will be discussed later. ρ_E, ρ_O, ρ_C and ρ_I are the environmental adjustment coefficients. Here $\rho_E = 0.35, \rho_O = 0.1, \rho_C = 80$ and $\rho_I = 10$.

Then experiments of sonar reading errors are carried out to analyze the \mathcal{E} of the mathematical sonar model. The results are shown in Tab.1. An object is placed in front of a fixed sonar sensor to survey the sonar readings. 20 sonar readings are recorded every 500 millimeters. The distance between object and sonar sensor is from 500 millimeters to 3000 millimeters. All errors in the range of 3000 millimeters are under 1%. So define the valid maximum R is 3000 millimeters and \mathcal{E} equals to $1\% \times R$.

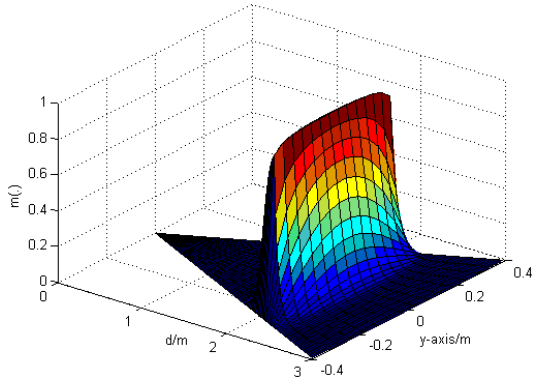
Table 1 Experimental sonar readings at different distances and relevant analysis

Actual distance (R/mm)	500	1000	1500	2000	2500	3000	
Sonar reading (mm)	502	997	1491	1987	2494	2988	
	501	997	1491	1987	2494	2988	
	501	997	1492	1987	2494	2987	
	501	997	1492	1987	2494	2987	
	501	997	1492	1987	2494	2987	
	501	998	1492	1987	2492	2988	
	501	998	1492	1987	2492	2988	
	502	998	1492	1987	2494	2988	
	502	998	1492	1987	2494	2988	
	502	998	1492	1987	2494	2988	
	502	998	1491	1986	2494	2991	
	502	998	1491	1986	2494	2991	
	502	998	1491	1987	2492	2988	
	502	998	1491	1987	2492	2988	
	502	997	1492	1987	2494	2988	
	502	997	1492	1987	2494	2988	
	502	997	1492	1987	2494	2988	
	502	997	1492	1987	2494	2988	
	Mean of errors (e_m /mm)	1.7	-8.3	-5.35	-13.1	-6.4	-11.7
	$ \frac{e_m}{R} \times 100\%$	0.34%	0.25%	0.56%	0.65%	0.26%	0.39%

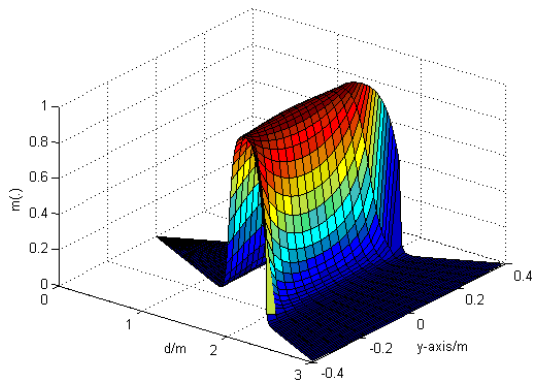
The analyses on the characteristics of gbbaf are shown in Figure 4. Considering the working principle of sonar, the nearer to the location of sonar reading, the greater the possibility of occupancy. Therefore the general basic belief assignment (gbba) of $m(\cdot)$ near the sonar reading R is much greater than any other places. In other words, the grid near R is probably occupied by some objects. But the gbba of $m(\cdot)$ is opposite. In the area near R the gbba of $m(\cdot)$ almost becomes zero, and in the sonar range, the farther away from R the greater the possibility of being empty. The conflicting mass $m(\cdot)$ is an uncertain part generated in the application of DSMT, it cannot be clearly ascribed to $m(\cdot)$ or $m(\cdot)$ and becomes greatest in the intersection of $m(\cdot)$ and $m(\cdot)$. At last, the gbba of $m(\cdot)$ becomes large in the areas beyond sonar range.



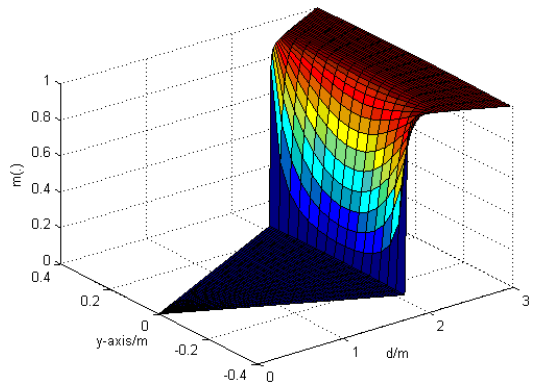
(a) gbba of $m(\cdot)$ when $R=2m$



(b) gbba of $m(\cdot)$ when $R=2m$



(c) gbba of $m(\cdot)$ when $R=2m$



(d) gbba of $m(\cdot)$ when $R=2m$

Figure 4 3D gbba distributing when $R=2m$

The conflicting factor between $m_1(\cdot)$ and $m_2(\cdot)$ follows the combining rules of Proportional Conflict Redistribution rule 2 (PCR2) [10] under the framework of DSMT.

4 Experiments

A user interface as a software platform for experiment is developed by us with Visual Studio 2008. The Pioneer 2-DXe mobile robot which is used in experiments has 16 sonar sensors fixed around it. Pioneer 2-DXe mobile robot is shown in Figure 5(a). Each sonar sensor is an evidence source. Initially, the discounting function for each sonar should be learnt through ANN. Take the first sonar data 502mm of Tab.1 for example, the sonar reading is treated as the midline of the sonar range ($\theta = 0$). The object is surveyed at the distance of 502mm but the actual distance is 500mm. Then four bba for the distance of 500mm are calculated (use Eq.(1-4), $R = 0.502$ and $d = 0.5$, the bba are $m(\theta_1) = 0.0086$, $m(\theta_2) = 0.9913$, $m(\theta_1 \cap \theta_2) = 0.0001$ and $m(\theta_1 \cup \theta_2) = 0$), and the actual bba for the distance of 500mm are $m(\theta_1) = 0$, $m(\theta_2) = 1$, $m(\theta_1 \cap \theta_2) = 0$ and $m(\theta_1 \cup \theta_2) = 0$. Then the vector [0.0086, 0.9913, 0.0001, 0] is the input of the ANN and the target output is [0, 1, 0, 0]. The data of Tab.1 can train an ANN for a sonar sensor. 16 ANN should be trained here for there are 16 sonar sensors.

There are many excellent ANN algorithms, but here we don't need a complex one and then the classical BP neural network with three layers is adopted. Both input layer and output layer have four neurons. The hidden layer includes five neural neurons. The training function is Levenberg-Marquardt back propagation because it is very fast. The activation function is the sigmoid function. The Performance function is Sum Squared Error (SSE). The learning rate is 0.1 and the error goal is 0.001. In order to enhance the precision, the input and output vectors are magnified 1000 times.

After training, another group of sonar readings are used to testify the validity of revision. The comparison between gbba without revision and gbba revised by BP neural network is as Tab. 2. The gbba revised by BP neural network have been normalized. The $m(\cdot)$ is the gbba of the grid at the actual distance. It is obviously that the BP neural network performs well.

An experiment field (size: 4840×3100 mm) is firstly created. The point of robot is treated as the coordinate origin of the global map. So robot is set to the pose of $(0, 0, 0^\circ)$. The third parameter is the deflection angle of robot. The robot must construct the dynamic environment model. Before exploring the environment, suppose the map is entirely unknown, that means $m(\theta_1 \cup \theta_2) = 1$ for each grid, and $m(\theta_1) = m(\theta_2) = m(\theta_1 \cap \theta_2) = 0$.

In the experiment, a person walks in the field all the time to represent the dynamic factor. The demonstration of dynamic map building is shown in Figure 5. The sectors in the built maps are the districts scanning by corresponding sonar sensors. The robot walks itself while a person moves beside it. In Figure 5, it is shown that the moving person is detected by sonar sensors of the robot. The locations of the moving person are marked by red circles. Obviously, the map is dynamically updated in time.

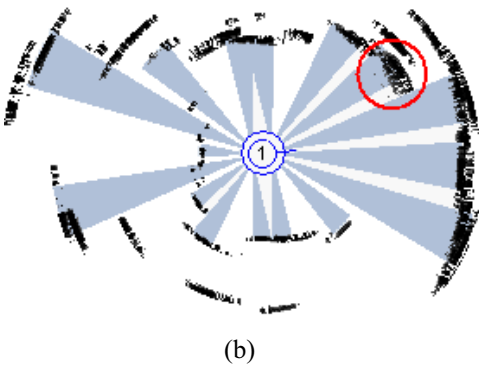
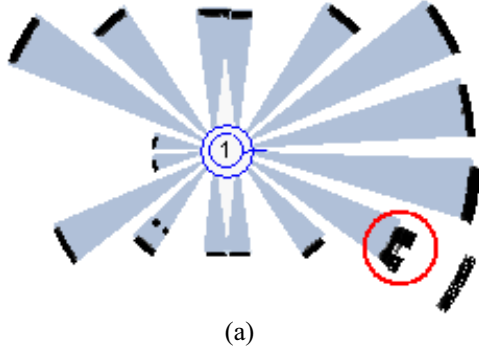


Figure 5 Dynamic map building with DSMT
(a)-(b) Moving person is detected by sonar sensors

An experiment field (size: 4840×3100 mm) is firstly created. The point of robot is treated as the coordinate origin of the global map. So robot is set to the pose of $(0,0,0^\circ)$. The third parameter is the deflection angle of robot. The robot must construct the dynamic environment model. Before exploring the environment, suppose the map is

entirely unknown, that means $m(\theta_1 \cup \theta_2) = 1$ for each grid, and $m(\theta_1) = m(\theta_2) = m(\theta_1 \cap \theta_2) = 0$.

In the experiment, a person walks in the field all the time to represent the dynamic factor. The demonstration of dynamic map building is shown in Figure 5. The sectors in the built maps are the districts scanning by corresponding sonar sensors. The robot walks itself while a person moves beside it. In Figure 5, it is shown that the moving person is detected by sonar sensors of the robot. The locations of the moving person are marked by red circles. Obviously, the map is dynamically updated in time.



Figure 6 Final building map

The final building map is shown in Figure 6 and the corresponding 3D map is shown in Figure 7 (the high of the lines denotes the belief assignment). The experimental result shows that the ERM based on DSMT can deal with these high conflicting and uncertain information perfectly. In unknown dynamic environment, the DSMT framework can draw accurate map after filtering the dynamic interferential factors and update the map in time (in Figure 5, it is obvious the map is dynamically updated real time). Outlines of objects and location are expressed clearly. The localization method is very efficient though it is so simple. There is few coordinate error in the created map.

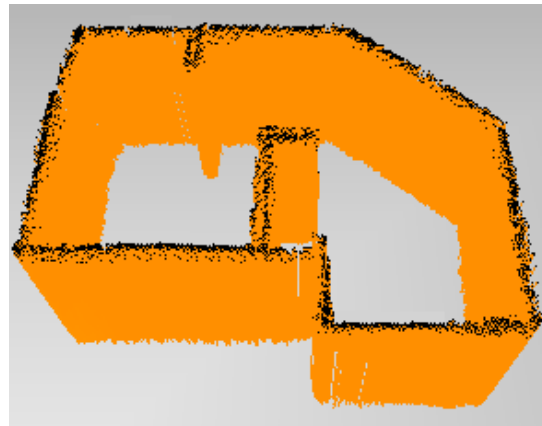


Figure 7 3D final map built by OpenGL

Compare with our previous work [8], it is obvious that after belief revising by ANN, the heights of the lines in Figure 7

are nearly the same. The shorter lines in [8] are revised perfectly. That is to say that there are no uncertainties.

5 Conclusions

This paper has proposed a mobile robot system with ERM based on DSMT for robot map building in an unknown dynamic environment. With the application of DSMT framework, the ERM is constructed, also a group of gbbaf functions is proposed for sonar sensor and the ANN is used to revise the sonar data. Through the result of experiment carried out with Pioneer 2-DX mobile robot, the mobile robot system with ERM based on DSMT is proved to be a valid system, especially for fusing imprecise, uncertain and even high conflicting information and building map accurately.

Acknowledgments

This work is supported by the National Natural Science Foundation of China (NSFC) under grant No. 60675028, this is greatly acknowledged.

References

- [1] S. Noykov, C. Roumenin. "Occupancy grids building by sonar and mobile robot". *Robotics and Autonomous Systems*, 2006, 55(2): 162-175.
- [2] L. Yenilmez, H. Temeltas. "A new approach to map building by sensor data fusion: sequential principal component-SPC method". *The International Journal of Advanced Manufacturing Technology*, 2007, 34(11): 168-178.
- [3] G. Grisetti, G. Tipaldi, C. Stachniss, W. Burgard, Daniele Nardi. "Fast and accurate SLAM with Rao-Blackwellized particle filters". *Robotics and Autonomous Systems*, 2007, 55(1): 30-38.
- [4] M. Begum, G.K.I. Mann, R.G. Gosine. "Integrated fuzzy logic and genetic algorithmic approach for simultaneous localization and mapping of mobile robots". *Applied Soft Computing*, 2008, 8(1):150-165.
- [5] J. Dezert. "Foundations for a new theory of plausible and paradoxical reasoning". *Information and Security*, 2002, 9: 13~57.
- [6] G. Shafer, *A Mathematical Theory of Evidence*, Princeton Univ. Press, Princeton, NJ, 1976.
- [7] J. Dezert, F. Smarandache, *Advances and Applications of DSMT for Information Fusion Vol.1*. Rehoboth: American Research Press, 2004.
- [8] P. Li, XH Huang, M. Wang. "Robot Map Building in Unknown Dynamic Environment Based on Hybrid Dezert-Smarandache Model". *Information Technology Journal*, 2009, 8(3): 284-292.
- [9] A. Elfes, H. Moravec, "High resolution maps from wide angle sonar", *IEEE Int. Conf. Robotics and Automation*. Leuven: IEEE. 1985, pp: 116-121.
- [10] J. Dezert, F.Smarandache, *Advances and Applications of DSMT for Information Fusion. Vol.2*. Rehoboth: American Research Press, 2006.

Table 2 Comparison between gbba without revision and gbba with revision

R : Sonar reading(mm) d : Actual distance(mm)		$R=502$ $d=500$	$R=996$ $d=1000$	$R=1493$ $d=1500$	$R=1988$ $d=2000$	$R=2495$ $d=2500$	$R=2987$ $d=3000$	AAD
$m(\theta_1)$	No revision	0.0086	0.0081	0.0079	0.0076	0.0075	0.0071	0.78%
	Revised	0.0000	0.0000	0.0000	0.0000	0.0000	0.0001	0.01%
$m(\theta_2)$	No revision	0.9912	0.9867	0.9680	0.9407	0.8991	0.8722	5.70%
	Revised	1.0000	1.0000	0.9999	0.9999	1.0000	0.9999	0.01%
$m(\theta_1 \cup \theta_2)$	No revision	0	0	0	0	0	0	0
	Revised	0	0	0	0	0	0	0
$m(\theta_1 \cap \theta_2)$	No revision	0.0001	0.0053	0.0242	0.0517	0.0934	0.1207	4.92%
	Revised	0	0	0	0	0	0	0